5-2011

Two dimensional modeling of wind effects on a bridge section using finite difference method

Jessica Carreiro
University of Arkansas, Fayetteville

Two Dimensional Modeling of Wind Effects on a Bridge Section Using Finite Difference Method

Two Dimensional Modeling of Wind Effects on a Bridge Section Using Finite Difference Method

A thesis submitted as partial requirement for the degree of

Bachelor of Science in Civil Engineering with Honors

By

Jessica Carreiro

April 2011

University of Arkansas

ABSTRACT

Wind effects on long span bridges are a major concern for bridge design. Wind acts as a dynamic load on the bridge deck causing the bridge to react in ways not accounted for in static load design. Attention to these effects increased tremendously after famous bridge collapses, such as the Tacoma Narrows Bridge in 1940. Due to this collapse and others, engineers were made painfully aware that wind phenomena, such as flutter and vortex shedding, can cause major structural damage if not considered in the design process. The solution for many years since has been to conduct wind tunnel tests on small scale models of bridges, which are both time consuming and expensive. In the last few decades, the capabilities of computers have increased exponentially to a point where it is feasible for engineers to develop a computer process that will produce the same values that could be found in a wind tunnel test.

This thesis begins to explore the time efficiency and viability of using a computer model based on the finite difference model (FDM) for solving the governing equations. The most typical computing method is the finite element method which has been thoroughly tested and produces reasonably comparable data to the wind tunnel tests that have also been performed. The Great Belt East Bridge (GBEB) is the subject of all the modeling done in both the wind tunnel and the computer simulations. The time required to run a finite difference method program is less than that required for the finite element method. The Strouhal number and coefficient of drag are observed to ascertain whether the FDM analysis results are sufficiently close to wind tunnel numbers for the GBEB. The results of this study indicate that FDM does not appear to generate reasonable values for C_d and S_t at the grid refinements simulated in this work.

This thesis is approved for
Recommendation to the
Honors Council

Thesis Director:

_____
Dr. R. Panneer Selvam

Thesis Committee:

_____
Dr. Kirk A. Grimmelsman

_____
Dr. Micah Hale

_____
Dr. Richard A. Coffman

THESIS DUPLICATE RELEASE

I hereby authorize the University of Arkansas Libraries to duplicate this Thesis when needed for research and/or scholarship.

Agreed _____
Jessica Carreiro

Refused _____
Jessica Carreiro

ACKNOWLEDGEMENTS

I would like to start by thanking Dr. R. Paneer Selvam for his offer to assist me in finding a project to work on and the opportunity to work on this project. I am thankful for the guidance and support he provided me as he introduced me to the subject matter and his patience as I stumbled through understanding the details. I am also thankful to my thesis defense committee members Dr. Kirk Grimmelsman, Dr. Micah Hale, and Dr. Rick Coffman for agreeing to serve on my committee and making very beneficial suggestions.

I would like to thank my family, especially both of my parents for their support and encouragement through the whole process as well as some helpful suggestions.

Finally, I would like to express gratitude to all of those not mentioned previously who gave me any form of support through the course of this project.

TABLE OF CONTENTS

Chapter 1

INTRODUCTION

1.1 Background

Bridges have been a necessity since the early days of civilization. Man has always needed a way to travel over difficult terrain to reach his destination. The advent of suspension bridges necessitated a modification in the design process because the structure is less rigid than short span bridges. The earliest suspension bridge spanning over 1,000 meters was the George Washington Bridge which was built within the last century (1931). The dynamic effects of wind could have on bridges wasn't a significant design consideration until the Tacoma Narrows Bridge collapsed in November 1940. Since its collapse, much effort has been taken to understand the multiple effects that wind flowing over bridges can have on the dynamic behavior of the bridge.

Over the last century, wind tunnel modeling has been the primary method for studying the dynamic effects of wind on structures. This method of observation is very effective; however, it can take 6-8 weeks to complete such a study and the approach is costly. In the last few decades the data processing power of computers has increased to such a level that modeling the flow of wind over a bridge is possible. Results that would take eight weeks to obtain from wind tunnel tests, take the computer only a few days to run (Govindaswamy & Selvam, 2001). Some complicated phenomena, such as tornado-structure interactions, are difficult to recreate in a wind tunnel, but can be easily simulated in a computer model. The time saved alone makes computer modeling worth investigating and improving. The results from computer modeling

have been compared to wind tunnel results and used to modify and improve the various computational methods.

1.2 Motivation

Much work has been done in the area of two dimensional computer analysis over the past couple of decades. As more research is done in this area, the computer modeling of structures will improve and can be established as a reasonably accurate alternative method for studying dynamic wind effects on structures. An essential goal of such research is to determine what computational method is the most comparable to wind tunnel results. There are two main computational methods that have been researched to date. The two methods for solving the computational fluid dynamics equations are the finite element method (FEM) and the finite difference method (FDM).

The FEM was reported to be a more accurate method than the FDM when the same grid spacing was used (Selvam 1998). However, the FDM analysis requires less computing time than the FEM analysis and could therefore save computing time if found to be sufficiently accurate at a closer grid spacing. If the FDM results become more accurate as the number of nodes around the bridge section is increased, the FDM would be a more time efficient method to use in modeling.

1.3 Objectives

The objective of this research is to validate the use of FDM modeling over other computational models by:

1. Modeling wind of $Re \approx 10^5$ using grids of increasing numbers of nodes.
2. Comparing Strouhal number and coefficient of drag from FDM analytical results to the values found by wind tunnel testing of the same bridge.
3. Determining whether the FDM model is more efficient in regards to computing time and if it is as viable as the FEM modeling approach.

Chapter 2

LITERATURE REVIEW

2.1 Aerodynamic Phenomena

Wind can be the source of significant dynamic forces on bridges. Long span bridges are less rigid and are therefore affected by dynamic wind forces more than rigid short span bridges. Over the last century, bridge failures have made engineers more aware of the volatile nature of long span bridges subjected to dynamic wind loads. Wind has both static and dynamic effects on structures. The static effects are very basic and can be dealt with in design in the same way any other static load is considered. The dynamic effects, however, cause more difficulty. A few of these effects are discussed in the following sections.

2.1.1 Flutter

This phenomenon is complex and until the last century was not completely understood or acknowledged by engineers. Flutter occurs due to a structure and wind interaction where the wind speed has passed the critical speed for flutter and negative damping develops. If a structure is experiencing an oscillation, positive damping will slowly decrease the amplitude of the displacement. On the other hand, flutter (negative damping) increases the amplitude of the oscillation as time continues. This means the displacement being experienced by any given point on a bridge will increase as the phenomenon continues. In Figure 2.1 a sinusoidal representation of both the positive and negative damping phenomena are shown. When a structure experiences flutter, failure can occur very quickly if it continues to build because of the increased stresses the bridge experiences from the increased movement.

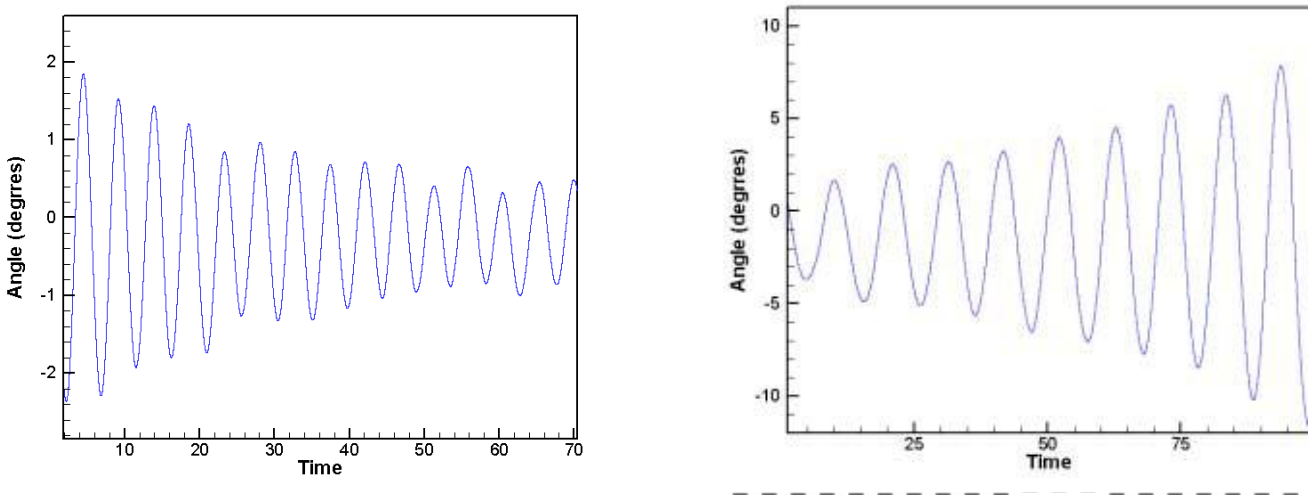

(a) (b)

Figure 2.1. Examples of (a) positive damping and (b) negative damping. (Govindaswamy, et al., 2001)

2.1.2 Buffeting

Buffeting is caused by turbulence in the air stream. The turbulence can cause the structure to experience torsional motion which quickly leads to failure. Turbulence in the air can be from two sources. The turbulence can just be preexisting in the air current as it approaches the structure. The other source could be turbulence created by the air moving over a nearby structure. When the buffeting occurs because of this source, it is known as wake buffeting.

2.1.3 Vortex Shedding

A major phenomenon that occurs as wind flows over the bridge deck is vortex shedding. As air flow hits the rigid bridge, the flow goes around the bridge by the flow separating around the bridge deck. Many studies of this specific phenomenon have been done using a circular cylinder as the rigid body. As the wind flows past the circular cylinder it creates two separate flows and with two different pressures on opposing sides of the bridge. The windward side of the bridge, the side the wind originates from, feels a pressure force from the wind and the leeward side, the opposite side from where the wind hits, feels a suction force. These two

different pressures cause the flow to create vortices as it flows past the far edge of the bridge (Simiu and Scanlan, 1996).

The Strouhal number is a quantity that describes this phenomenon and it is based on the lift forces that the bridge experiences while the wind flow is occurring. The Strouhal number is also heavily dependent on the Reynold's number associated with the wind flow. These three factors are described in more detail in Section 2.2.

2.2 Quantified Flow Characteristics

The flow of a fluid around a bridge is best modeled as the flow around a bluff body. A bluff body is a body that is not streamlined and forces the flow to separate completely as it flows around the body. The body forces the flow in such a way that turbulence is created within the flow. The group of equations that mathematically approximates this flow is called computational fluid dynamics (CFD).

These equations include the Navier-Stokes equation that is typically solved using the FEM or FDM methods. The behavior of the flow is determined by two different groups of factors. The Reynold's number associated with the flow is a determining factor and the roughness of the body is an influencing factor (Joshi, 2010). This means that the Reynold's number is the main factor that determines flow, but the flow is altered in a smaller way by the roughness of the body which is in the path of the flow. When these factors are known the flow can be classified more easily and therefore the effects more easily determined.

2.1.1 Reynold's Number

The Reynold's Number (Re) is a dimensionless measure of the ratio of the inertial forces to the viscous forces. The following equation is used to calculate the Reynold's number:

$$Re = \frac{V_{avg}D}{\upsilon}$$

Where V_{avg}, the average velocity of fluid flow, and D, the characteristic length, are the components that make up the inertial forces and υ, the kinematic viscosity, is representative of the viscous forces.

The critical Reynold's number region, the range between laminar and turbulent flows, differs according to the shape of the body obstructing the flow. For bluff bridge deck the critical Reynold's number is about 10^6. This work uses a Reynold's number of 10^5, which is considered a low Reynold's number (Schewe & Larsen, 1998).

2.1.2 Coefficient of Lift

The coefficient of lift,C_L, is a dimensionless measure of resistance due to the lift on the bridge due to lift forces that are acting. The equation to determine the coefficient of lift is:

$$C_L = \frac{2F_L}{\rho V^2 A}$$

Where F_L is the lift force which acts perpendicular to the flow of velocity (Figure 2.2), ρ is the mass density of the fluid, V is the velocity if the fluid, and A is the area.

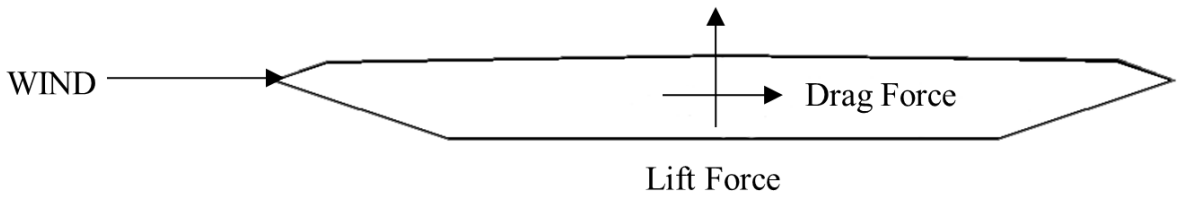

Figure 2.2. Drag and lift forces on the Great Belt East Bridge generated by wind

The above figure illustrates the direction the lift force acts on a bridge. The lift force acts perpendicular to the force of the wind on the bridge and the application of the lift force oscillates. The frequency at which the lift force acts on the bridge factors into the calculation of the Strouhal number, Section 2.1.4.

2.1.3 Coefficient of Drag

The coefficient of drag is the same basic concept as the lift coefficient.

$$C_D = \frac{2F_D}{\rho V^2 A}$$

Where F_D is the drag force which acts in the direction of the flow of velocity, ρ is the mass density of the fluid, V is the velocity if the fluid, and A is the area.

As the wind flows over the bridge a drag force is developed in the same direction of the wind velocity. The drag force is also perpendicular to the direction of the lift force, Figure 2.2.

2.1.4 Strouhal Number

The Strouhal Number is another dimensionless quantity and is equal to the characteristic length divided by the product of the period of the vortex shedding and the velocity of flow, as seen in the following equation:

$$S_t = \frac{D}{TV} = \frac{fH}{V}$$

Where S_t is the Strouhal number, T is the period of the lift forces, V is the flow velocity, H is the height of the bridge cross section, and f is the frequency of the vortex shedding ($f = \frac{1}{T}$), the lift forces.

The trend is that the Strouhal number increases as the Reynold's number increases, although some variance occurs at higher Reynold's numbers as seen in the Figure 2.3.

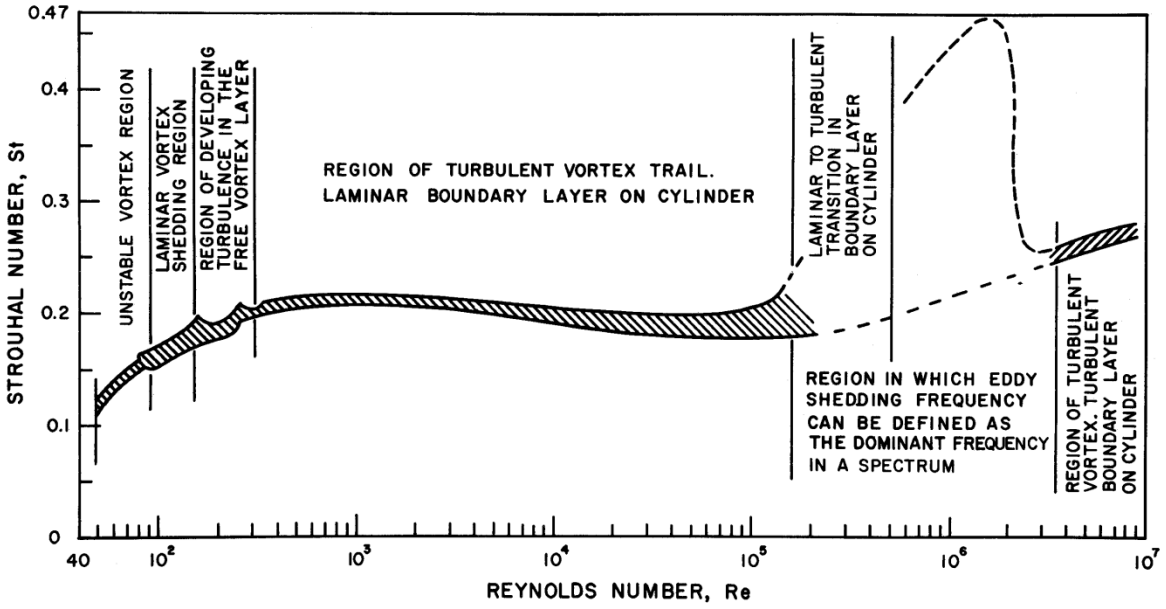

Figure 2.3. Reynold's Number Relationship to Strouhal Number (Lienhard, 1966)

Chapter 3

COMPUTER MODELING

3.1 Bridge Section

The bridge section used in all modeling for this work is a section of the Great Belt East Bridge (GBEB). This bridge was built in Denmark to connect the island on which lies its capital, Copenhagen, to Sprogo and acts as an important trade route. The GBEB opened to use in 1998 and its longest span is 1,624 meters long (Storebaelt). The cross section used for modeling is taken from the long span of the bridge, Figure 3.1.

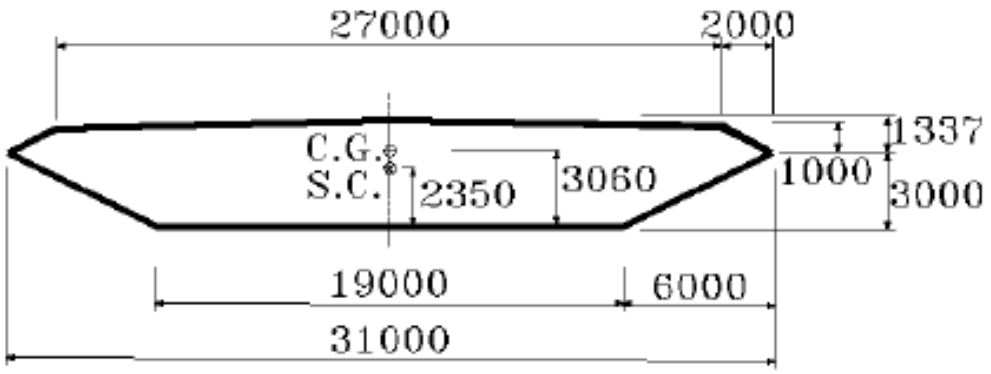

Figure 3.1. Cross section of the suspension span of the Great Belt East Bridge (GBEB), all dimensions shown in mm. (Walther, 1994).

3.2 Computer Modeling Overview

The cross section is taken as a dimensionless unit width of B as a step to make the computations and the program simpler. The initial step in modeling the flow of wind over the GBEB cross section is to create a space in which all the flow would be computed and modeled. A cross section of space surrounding the bridge cross section is determined in such a way to allow all the variations in flow of the wind to be seen in the model. There is a clearance of 5B above and below the vertical centerline of the bridge cross section. An approach distance of 4B

is given before the initial edge of the bridge and a horizontal space four times the length of the bridge is allowed past the far edge of the bridge. The modeling space is shown in Figure 3.2.

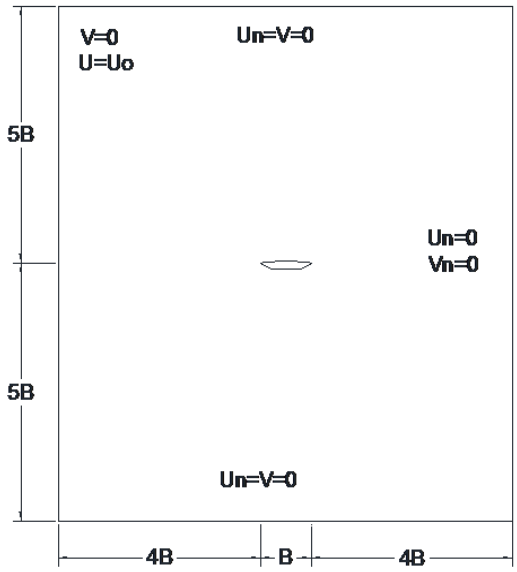

Figure 3.2. Modeling space for GBEB section for FDM computations

The approach velocity of the wind traveling over the first distance of 4B is made to be a unit velocity of 1 in the x direction so that the output of the model can be easily adjusted for any case. All other velocities are computed relative to the initial velocity. The other boundary conditions can be seen in Figure 3.2.

3.3 Grid Generation

Grid generation is an important component in the modeling of flow around bridges. The grid determines at what points information is computed. The grid spacing along the border of the bridge is the most important, because the flow at the bridge boundary is the most important for analysis (Selvam, et al., 2010). In this work a grid spacing of 0.00026B is used and the number of nodes around the bridge is used to differentiate between the three different grids used.

The number of nodes in the generated grid determines the accuracy of the coefficient of drag and the Strouhal number calculated from the model output. As the refinement of the grid increases, a clearer and more accurate model of the behavior of the flow of the wind is given by the model. The increase in nodes can dramatically change the pattern of the vortices and the accuracy of the resulting coefficient of drag. Consequently as the nodes around the bridge increase so does the time to run the computer model (Selvam, 2010).

The grid is a radially expanding grid that has its smallest spacings along the boundary of the bridge. This type of grid is used because the information close to the bridge is the most important. Calculations need not be as closely spaced as the distance from the bridge increases. A typical grid is shown in Figure 3.3.

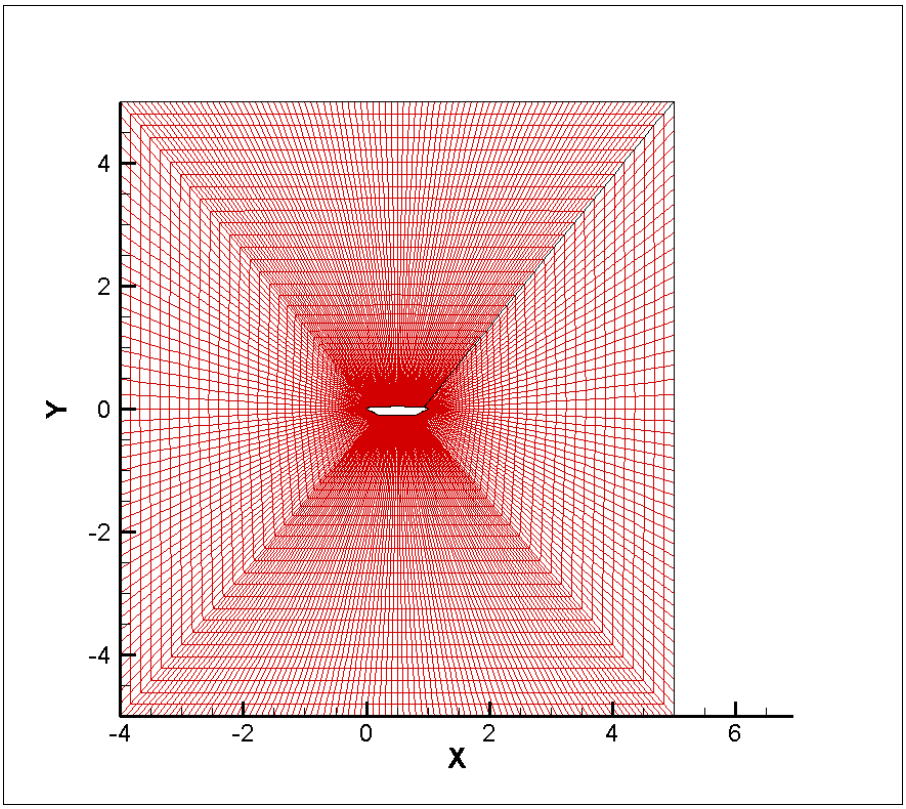

Figure 3.3. The grid system for the GBEB cross section

3.4 Numerical Methods

The numerical modeling of the wind flow is determined by the Navier-Stokes equations for a fluid that is assumed to be incompressible and viscous. There are a couple methods that are used to solve the Navier-Stokes equations, finite difference method (FDM) and the finite element method (FEM). Much work has been done modeling using the FEM method in two dimensional analysis. It has been reported that the FEM method is more accurate compared to the FDM method for a given grid spacing (Selvam, 1998). However, the computational time required for computer modeling based on the FDM method is much less than that required for the FEM method. This work looks at increasing the amount of nodes around the bridge with a very small grid spacing of 0.00026B, which was shown to be sufficiently small for the Reynold's number used by Selvam and Patterson (1993).

3.5 Calculation Implementation

The implementation of all these separate procedures involves 5 different programs and is an involved process. The final ouput includes the coefficient of lift, the coefficient of drag, and the vorticity. The procedure used to obtain the data is outlined step by step in the Appendix. The visualizations of the data are created by loading the output files into Tecplot.

Chapter 4

RESULTS

4.1 General Remarks

The analysis for the bridge cross section is done with a computer model that uses the finite difference method (FDM) to solve the Navier-Stokes equations. The input and execution process used to obtain the data presented in this chapter is outlined in the Appendix. The same model is run using three different grid refinements. The grid dimensions are 273x79, 547x79, and 819x79. The total number of nodes around the perimeter of the bridge for the grids one, two and three are 273, 547, and 819 nodes respectively. These grids all have a grid spacing of 0.00026B. The number of tangential grid points is not varied in this work because of time restrictions. The computations vary depending on the number of grid points. The small variations between the different grids at the beginning of the run time are amplified as time continues to flow. Each grid is run for two different time durations, a non-dimensional time of 20 and 60. A significant amount of time, 10s, is cut out of the 20s duration to allow the calculations to begin a reasonable constant oscillation so that the frequency plot can be generated as accurately as the data will allow. Since half of the time is dismissed the second run, the 60s duration, is necessary to obtain reasonable data to compute the frequency.

The results from all three grids are found and calculated individually. The calculated results are compared to wind tunnel experiments and past results from other researchers. There are plots included of the vorticity and vector diagrams for each of the grids. The coefficients of drag and frequency plots are also reported.

4.2 Results

It is assumed that the bridge cross section is rigidly fixed and no rotational or translational displacements can take place. There are three different grids used; the difference between each being only the number of nodes around the perimeter of the bridge. The original grid is 273x79. This means there are 273 points around the perimeter of the bridge and in the tangential direction there are 79 points moving toward the outermost boundary. This grid uses the spacing of 0.00026B. This means that the distance from the bridge boundary to the nearest grid line is 0.00026B. The grid spacing is measured relative to the width of the bridge section, B.

The output is based on the following inputs: Reynold's number, grid spacing, number of nodes, time step, and number of time steps. For this work the time step used is 0.001 seconds and the total run time is 20 and 60 seconds. The turbulence of the wind is determined by the Reynold's number, which is 10^5 for this work. A user manual for the computer input and process is included in the Appendix.

The results that come directly from the computer computations are the coefficient of drag over the duration of time and the vector/vorticity plots. The actual coefficient of drag is calculated using a program that averages the data points over the duration, excepting the first 10s to allow the data to regulate. The remaining time and corresponding coefficient of drag data serve as input into the averaging program.

The coefficient of lift is also given and the frequencies of this coefficient with the greatest amplitudes determine the Strouhal number. The coefficients of lift are used as input into a computer program that can extract the frequency and amplitude. Those frequencies with

the greatest amplitude are used to calculate the Strouhal number using the following equation as explained in section 2.1.2:

$$St = \frac{fH}{V} = 0.14f$$

This equation can be reduced as shown because the velocity is 1 and the height of the bridge cross section is 0.14 of B. All the calculated quantities are summarized in Table 4.1 and Table 4.2.

Table 4.1. Summary of all 3 grid configuration results for 20s duration

Grid	Points	Spacing	Computation Time	Frequency (f)	S_t=.14f	C_d
1	273x79	0.00026	30 min	1.5	0.21	.0615
2	547x79	0.00026	80 min	1.6	0.224	.0537
3	819x79	0.00026	167 min	2.2	0.308	.0553
FEM	800x35	0.00026	> 1 day	1.07 & 1.4	0.15 & 0.196	0.0731
Wind Tunnel	-	-		-	.11 & .158	.077

Table 4.2. Summary of all 3 grid configuration results for 60s duration

Grid	Points	Spacing	Computation Time	Frequency (f)	S_t=.14f	C_d
1	273x79	0.00026	76 min	0.3, 1.4, 1.7 & 1.5	.042 & 0.21	.0587
2	547x79	0.00026	219 min	0.2, 1.89, & 1.6	0.028 ,0.265, & 0.224	.0531
3	819x79	0.00026	485 min	2.1 & 2.2	0.294 & 0.308	.0538
FEM	800	0.00026	> 1 day	1.07 & 1.4	0.15 & 0.196	0.0731
Wind Tunnel	-	-		-	.11 & .158	.077

The difference between the output value and the wind tunnel value for C_d increases as the number of nodes around the perimeter of the bridge increases from 273 nodes to 547 nodes. Then grid 3 compared to the wind tunnel value has a smaller difference yet still greater than the C_d from grid 1. The outputs for C_d for both duration periods appear to possibly be converging. It seems from the data that the grid refinements give a S_t that increases with each grid refinement

moving further away from the wind tunnel value. One would expect the trend to be that as the grid is refined the S_t and C_d will approach the wind tunnel values. The cause of this break from expectations could possibly be due to a lack of refinement of grid points in the tangential direction, which were not refined due to time restraints.

The computation time for all of the grid combinations is significantly smaller than the computation time for the FEM method. In fact, the computation time for the most refined FDM grid is a little over a third of the time to run the FEM simulation. This is a huge advantage of the FDM over the FEM, if only the data was reasonable to use.

The following graphs are representative of each grid configuration and time duration showing the vorticity, velocity vector plot, the coefficient of drag, and the frequency of the coefficient of lift.

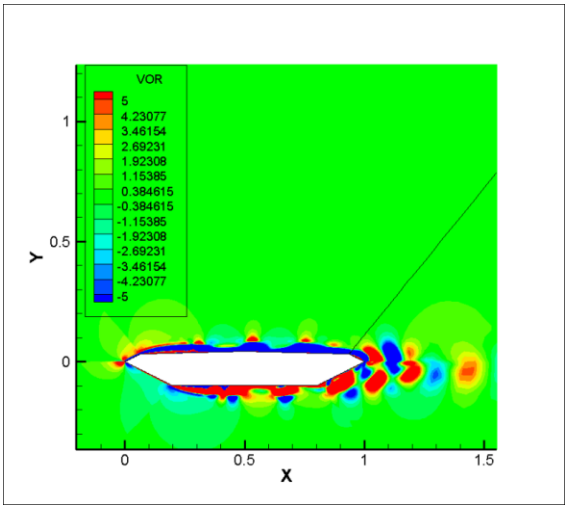

(a)

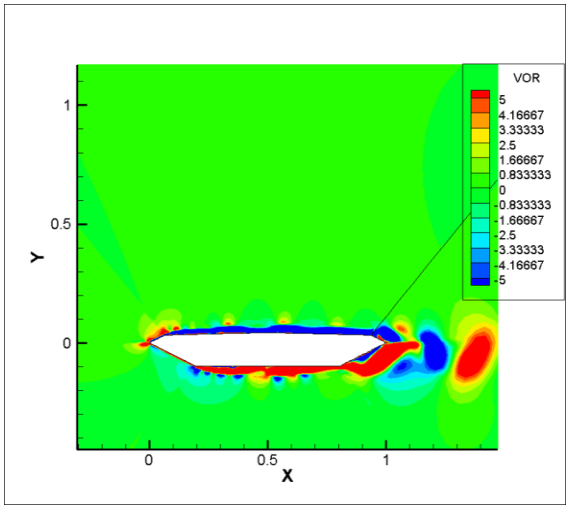

(b)

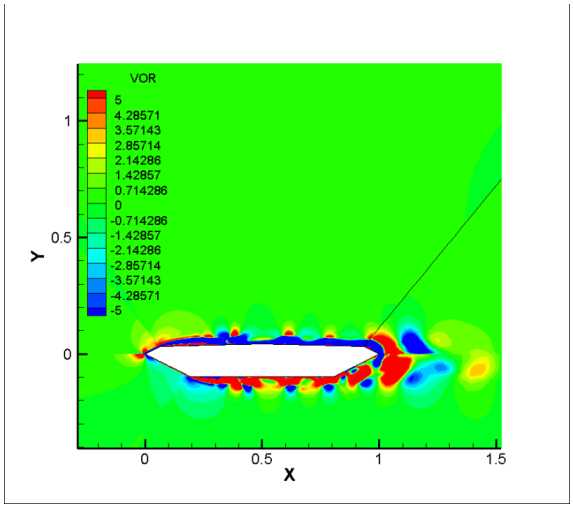

(c)

Figure 4.1. Vorticity contours at the end of non-dimensional time of 20 for different grid configurations (a) 273 nodes, (b) 547 nodes, and (c) 819 nodes.

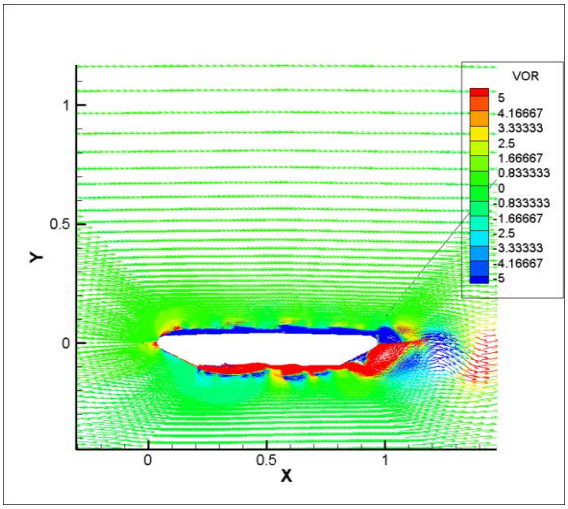

(a)

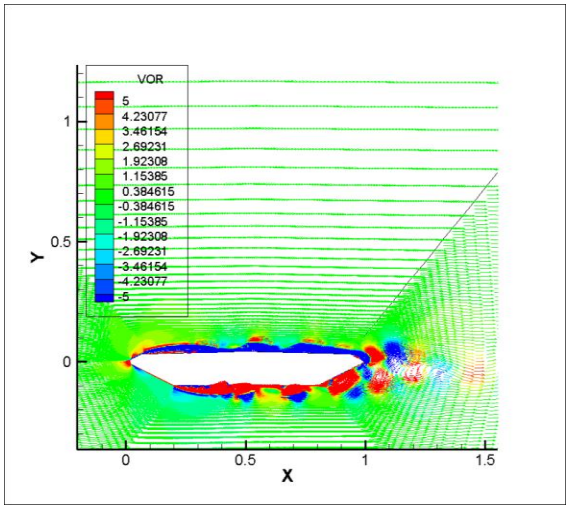

(b)

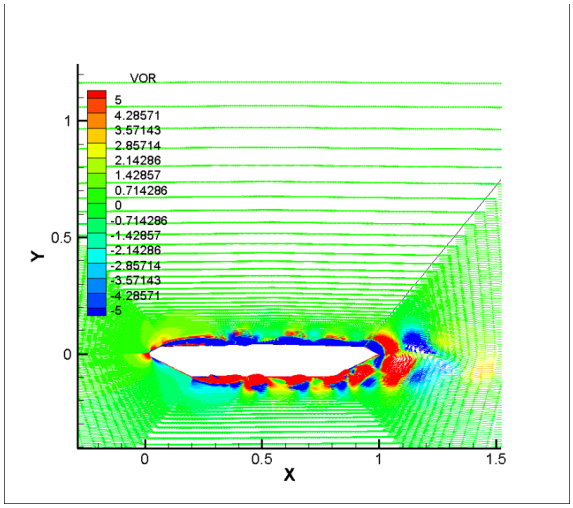

(c)

Figure 4.2. Velocity vector diagrams at the end of non-dimensional time of 20 for different grid configurations (a) 273 nodes, (b) 547 nodes, and (c) 819 nodes.

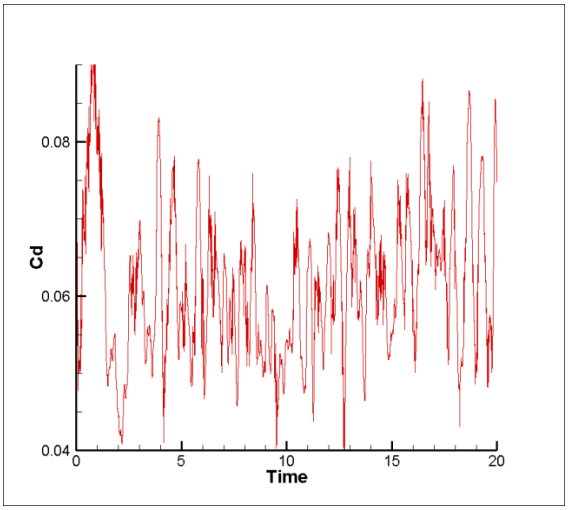

(a)

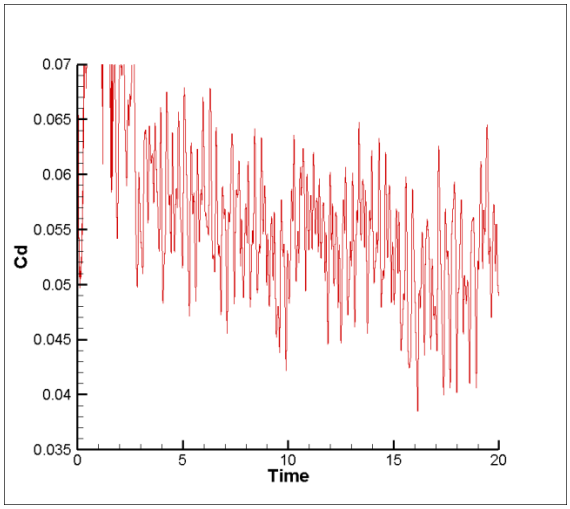

(b)

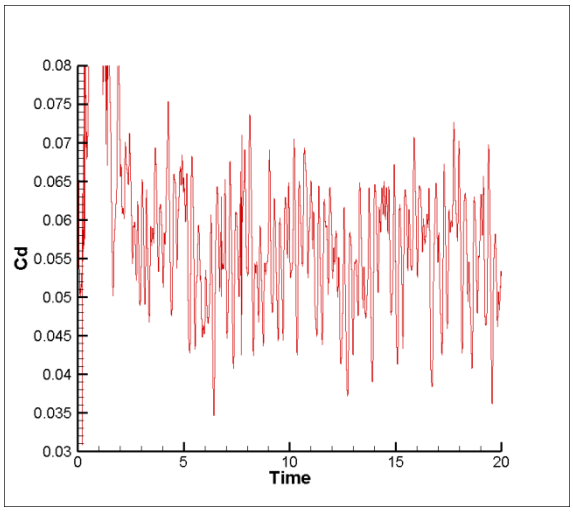

(c)

Figure 4.3. Coefficient of drag over the non-dimensional time of 20 for different grid configurations (a) 273 nodes, (b) 547 nodes, and (c) 819 nodes.

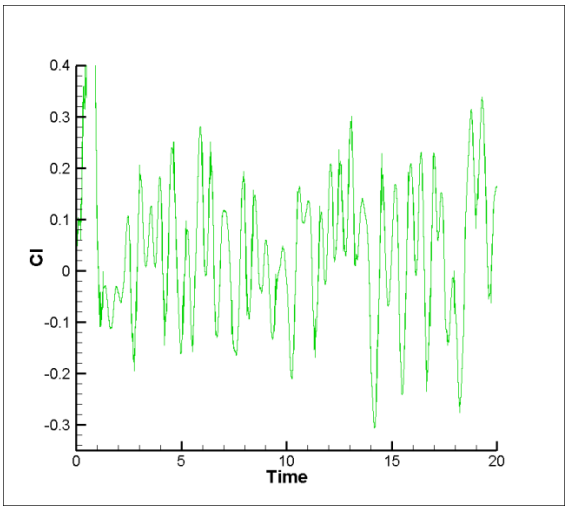

(a)

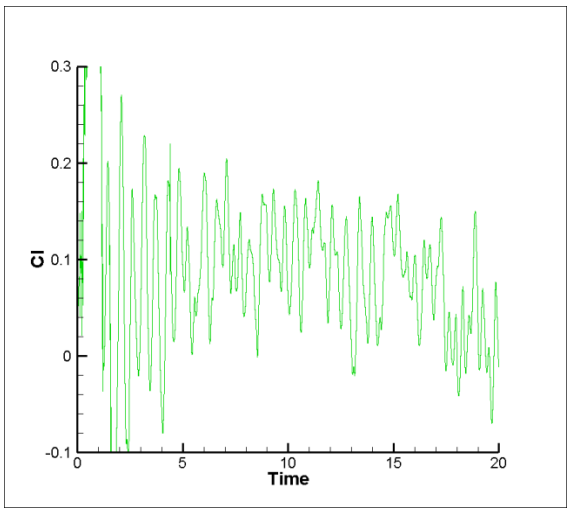

(b)

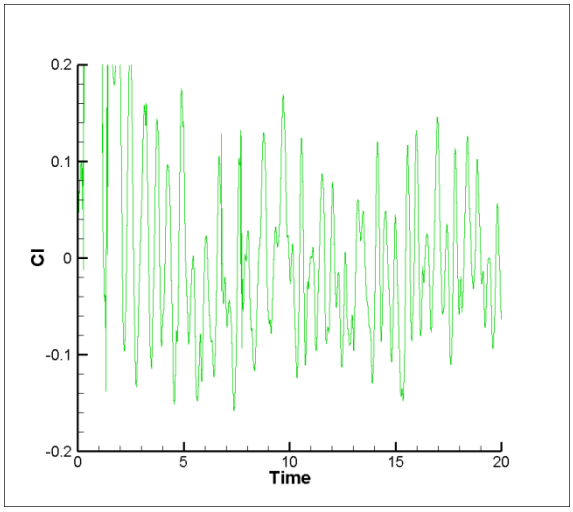

(c)

Figure 4.4. Coefficient of lift over the non-dimensional time of 20 for different grid configurations (a) 273 nodes, (b) 547 nodes, and (c) 819 nodes.

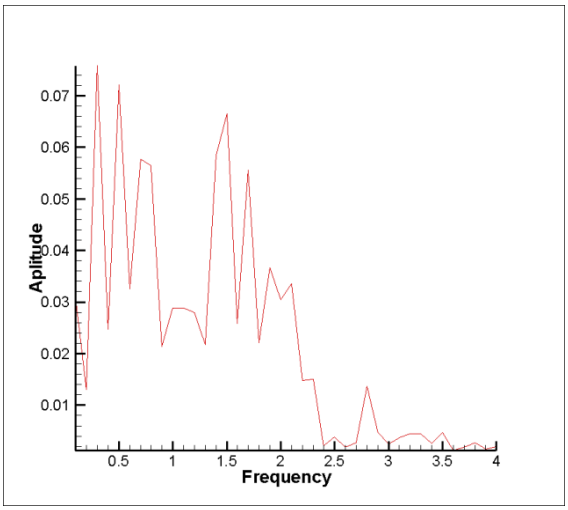

(a)

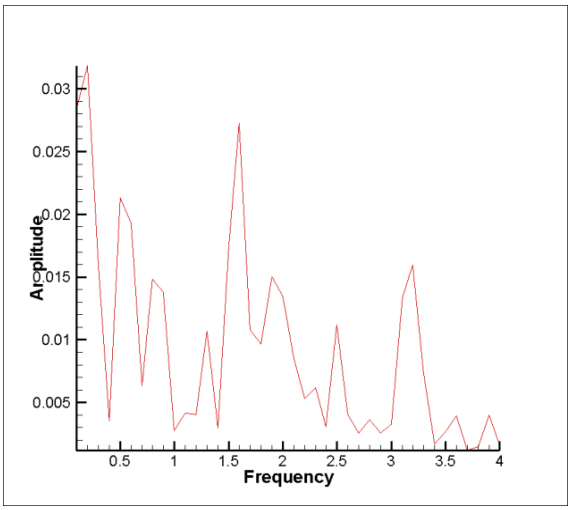

(b)

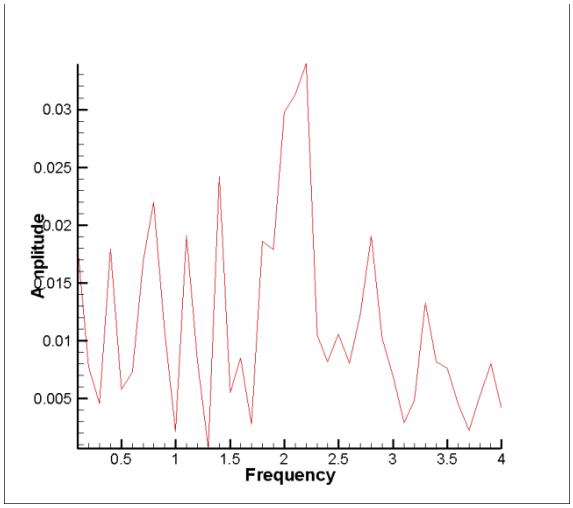

(c)

Figure 4.5. Frequency spectrum of the lift forces for different grid configurations at a 20s duration (a) 273 nodes, (b) 547 nodes, and (c) 819 nodes.

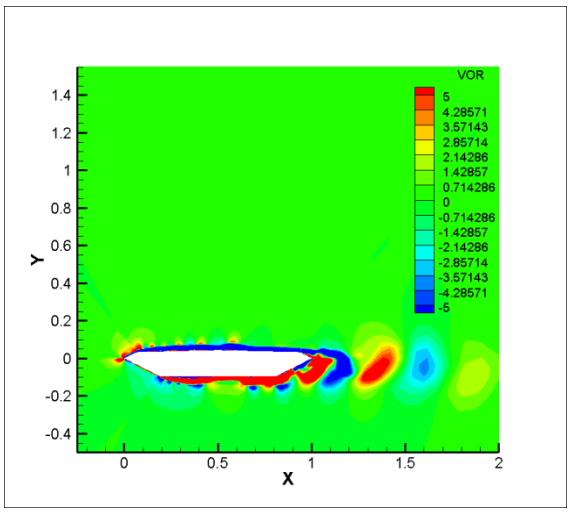

(a)

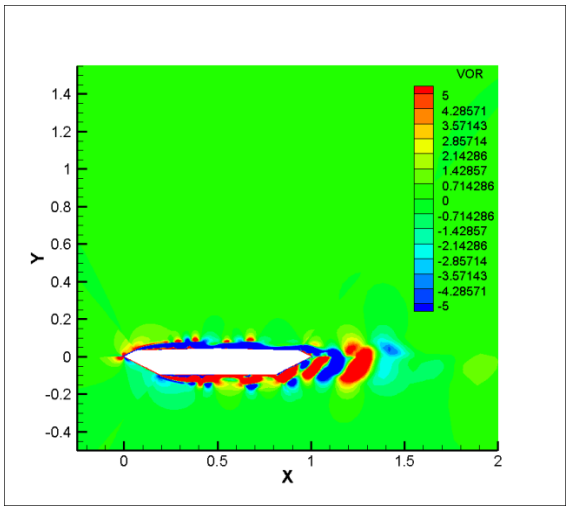

(b)

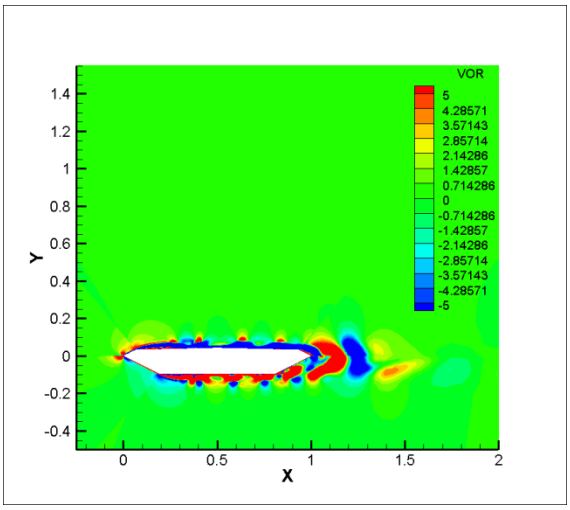

(c)

Figure 4.6. Vorticity contours at the end of non-dimensional time of 60 for different grid configurations (a) 273 nodes, (b) 547 nodes, and (c) 819 nodes.

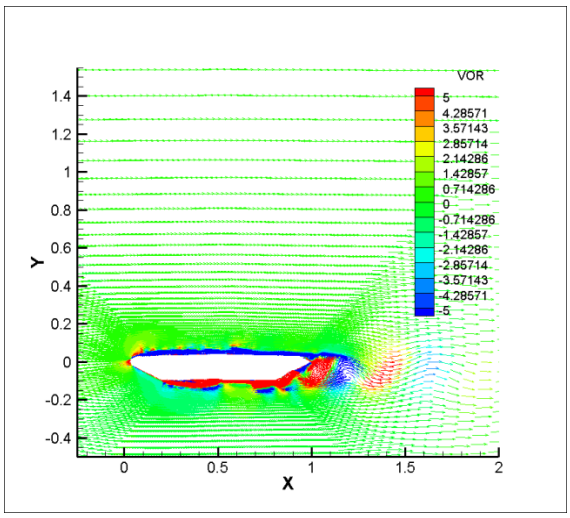

(a)

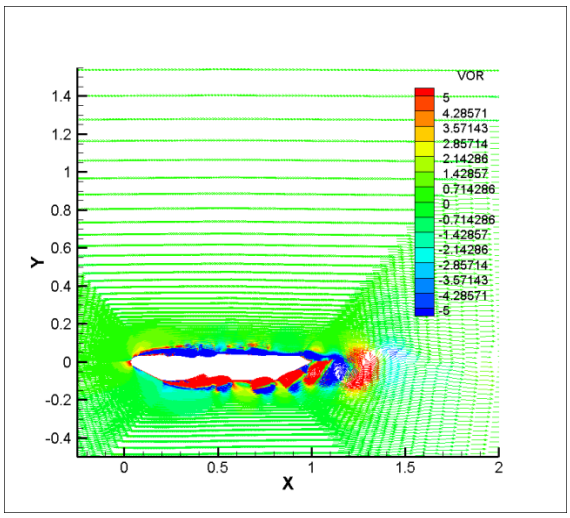

(b)

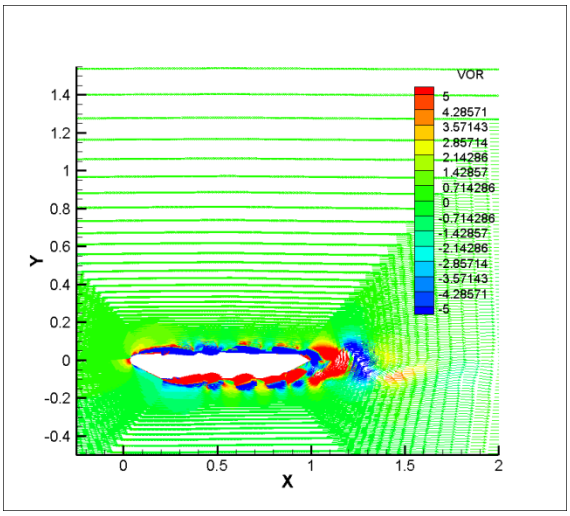

(c)

Figure 4.7. Velocity vector diagrams at the end of non-dimensional time of 60 for different grid configurations (a) 273 nodes, (b) 547 nodes, and (c) 819 nodes.

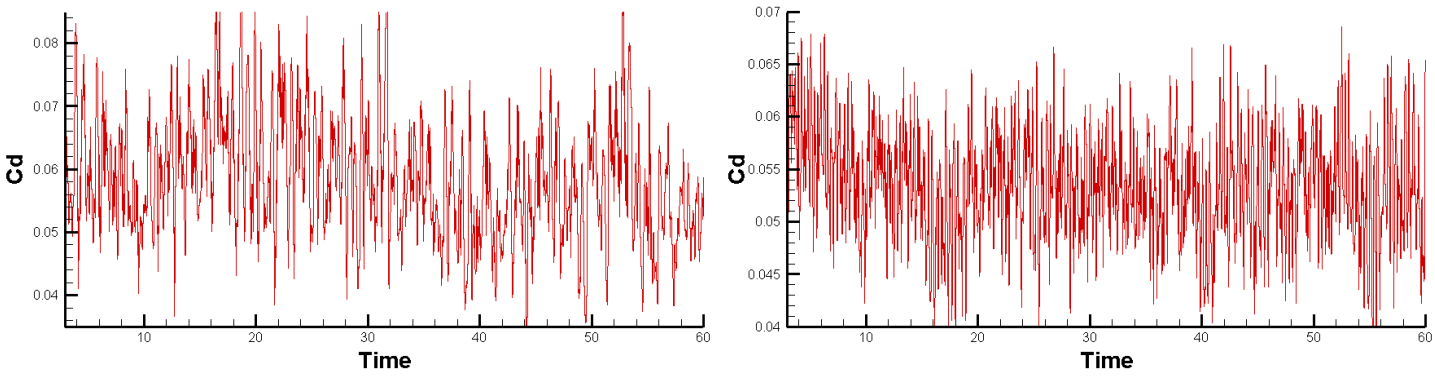

(a) (b)

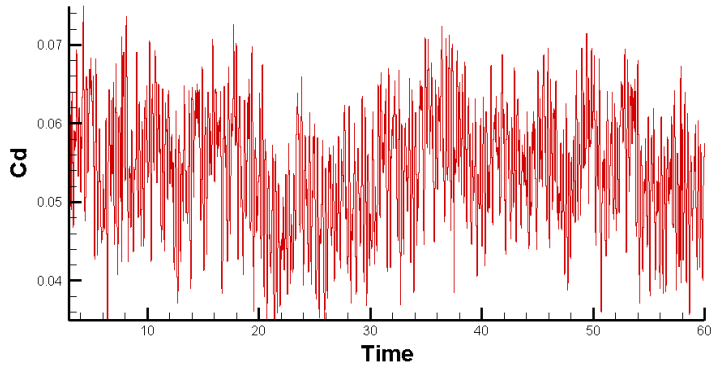

(c)

Figure 4.8. Coefficient of drag over the non-dimensional time of 60 for different grid configurations (a) 273 nodes, (b) 547 nodes, and (c) 819 nodes.

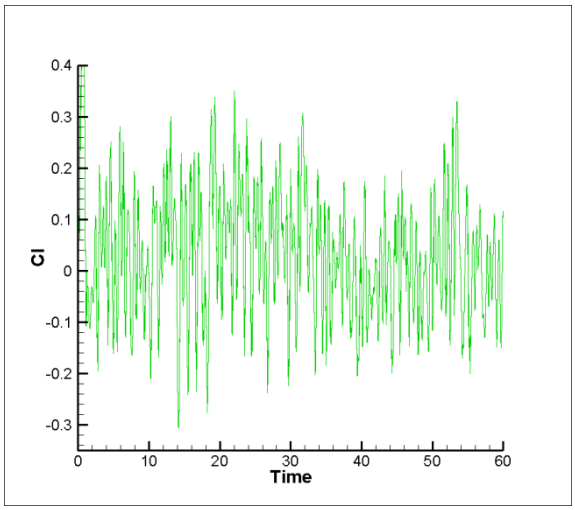

(a)

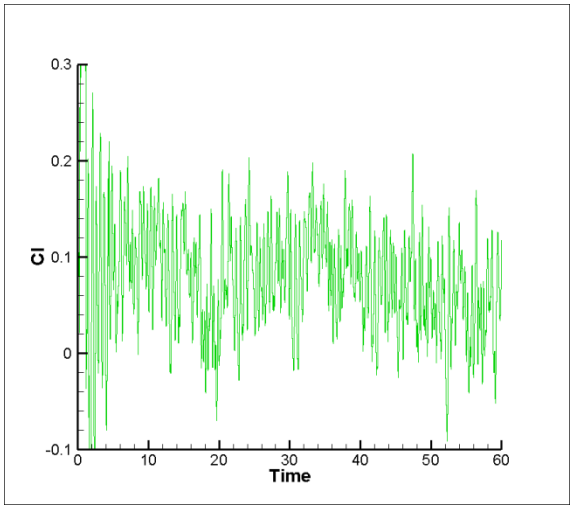

(b)

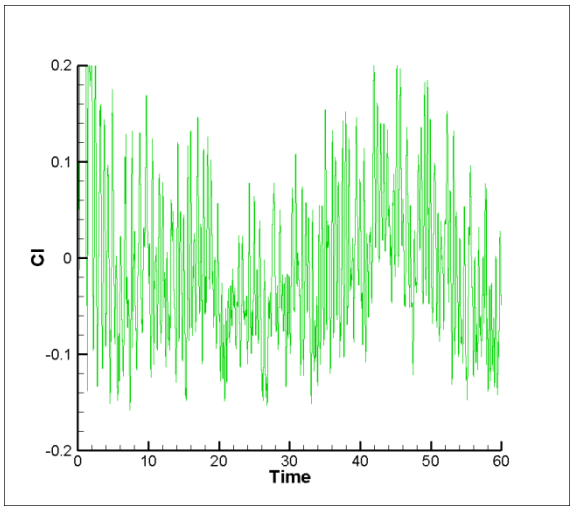

(c)

Figure 4.9. Coefficient of lift over the non-dimensional time of 60 for different grid configurations (a) 273 nodes, (b) 547 nodes, and (c) 819 nodes.

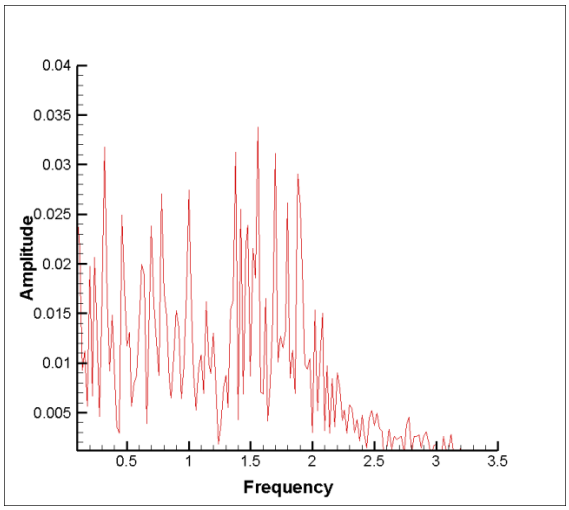

(a)

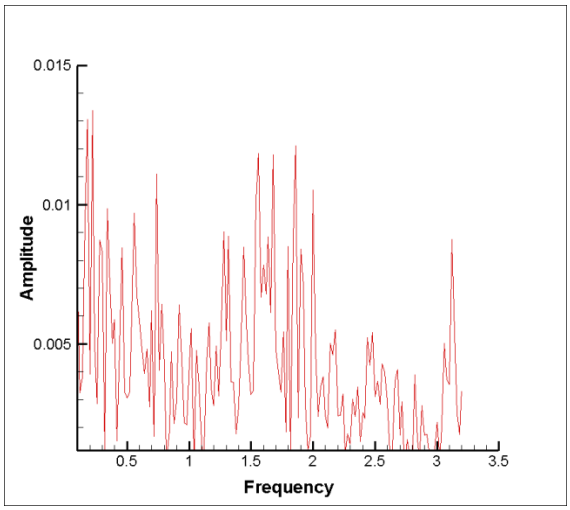

(b)

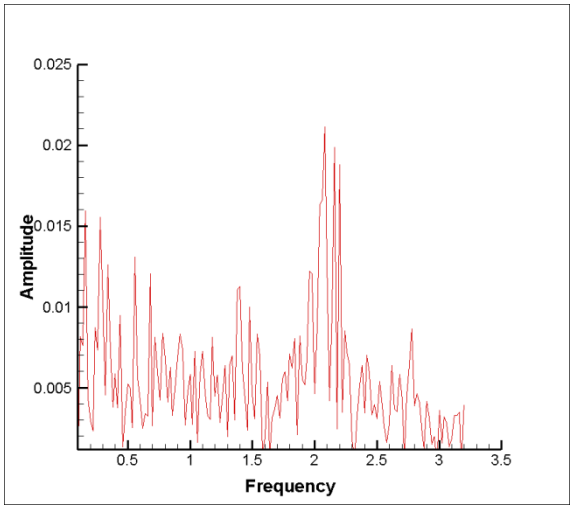

(c)

Figure 4.10. Frequency spectrum of the lift forces for different grid configurations at a 60s duration (a) 273 nodes, (b) 547 nodes, and (c) 819 nodes.

Chapter 5

CONCLUSIONS

5.1 Summary

The need for computational wind analysis was briefly explored as was the theoretical and mathematical basis for the analysis that is performed by the computer using the Finite Difference Method. A brief discussion was given on the advantages that a FDM method program would have over a FEM method if it could be shown to produce reasonable numbers.

The wind flow over the GBEB is shown using a FDM based simulation for three grids with various amounts of tangential nodes, the number of nodes around the boundary of the bridge. Two durations of the non-dimensional time of 20 and 60 respectively are included to be sure enough time is simulated. The coefficient of drag and the Strouhal number for each simulation is presented based on the data obtained from the simulation.

5.2 Conclusions

According to the data collected the FDM method of computer analysis is not more accurate than the FEM method. However, the computational time for the FDM method is significantly lower than for the FEM method. Therefore, more investigation into the FDM method of computation is worthwhile. The grid refinement of the nodes around the boundary of the bridge did not produce a convergence to the wind tunnel numbers as was expected. However, Grid 3 increased as if converging toward the wind tunnel value of C_d, perhaps even further refinement of the bridge boundary nodes would have revealed a trend toward the wind tunnel numbers.

The values most closely resembling the wind tunnel values for the FEM method (Selvam, 2010) were from the grid that was the most well refined radially as well as

tangentially. If this tangential refinement was applied to the FDM, perhaps it would give values more closely resembling the wind tunnel values. Perhaps this refinement will find the FDM method to produce reasonable values. If feasible values are found, the FDM method would be preferable because it would take about a third the computation time.

REFERENCES

Bosch, H., Patro, S.K., Selvam, R.P., (2007), "Adaptive FEM for Bridge Aerodynamics", [PowerPoint slides], Retrieved from file.

Govindaswamy, S., and Selvam, R.P., (2001)," A Report on Aeroelastic Analysis of Bridge Girder Section Using Computer Modeling", Department of Civil Engineering, University of Arkansas, Fayetteville, 2001. Report for Mack Blackwell Transportation Center.

Joshi, R., (2010), "Effect of Three Dimensionality on the Vortical Structures Behind a Bridge Deck Section", Department of Civil Eng., University of Arkansas, Fayetteville, Masters Thesis.

Lienhard, J.H., (1966), "Synopsis of lift, drag and vortex frequency data for rigid circular cylinder",Washing State Univ., Coll. Eng., Research div. Bull. 300

Schewe, G.and Larsen, A.,(1998), "Reynolds number effects in the flow around a bluff bridge deck cross section", *J. Wind Eng. Ind. Aerodyn.* **74–76** (1998), pp. 829–838.

Selvam, R.P. (1992), "Computation of Pressures on Texas Tech Building", *J. Wind Engineering and Industrial Aerodynamics*, 43, 1619-1627.

Selvam, R. P., (2010), "Building and Bridge Aerodynamics Using Computational Wind Engineering", **International Workshop on Wind Engineering Research and Practice**, Charlotte, NC..

Selvam, R. P., Bosch, H. and Joshi, R., (2010)," Comparison of 2D and 3D CFD Modeling of Bridge Aerodynamics", **The Fifth International Symposium on CWE,** Chapel Hill, NC.

Simiu, E., and Scanlan, R.H., (1996), "**Wind effects on Structures",** Third edition, Wiley Interscience, New York.

Storebaelt**,** Storebaelt: Sund Belt. *Facts and History,* [Online] [Cited: February 22, 2011.] http://www.storebaelt.dk/english/bridge.

Walther, J. H., (1994), "Discrete vortex method for 2D flow past bodies of arbitrary shape undergoing prescribed rotary and translational motion", **Ph.D. Thesis**, **Department of fluid mechanics, Technical University of Denmark**, Denmark.

APPENDIX

This appendix is a guide to data preparation and using the various programs/codes to reach the final outcome of S_t and C_d. Some codes can be used on any computer; others have large computing needs and must run through a Unix/Linux system. This work accessed such processors through SSH Secure Shell Client through the University of Arkansas.

1) Create tangential points

   Program: rdist.f

   This program outputs the information about the tangential grid lines. The output is used in the mrcyl.txt file used to create the modeling space. A sample of the output is included below:

0.0000000E+00 0.5000000E-03 0.1050000E-02 0.1655000E-02 0.2320500E-02
0.3052550E-02 0.3857805E-02 0.4743586E-02 0.5717945E-02 0.6789740E-02
0.7968714E-02 0.9265586E-02 0.1069214E-01 0.1226136E-01 0.1398749E-01
0.1588624E-01 0.1797487E-01 0.2027236E-01 0.2279959E-01 0.2557955E-01
0.2863751E-01 0.3200126E-01 0.3570139E-01 0.3977153E-01 0.4424868E-01
0.4917355E-01 0.5459090E-01 0.6055000E-01 0.6710500E-01 0.7431550E-01
0.8224705E-01 0.9097175E-01 0.1005689E+00 0.1111258E+00 0.1227384E+00
0.1355123E+00 0.1495635E+00 0.1650198E+00 0.1820218E+00 0.2007240E+00
0.2212964E+00 0.2439261E+00 0.2688187E+00 0.2962005E+00 0.3263206E+00
0.3594527E+00 0.3958980E+00 0.4359878E+00 0.4800866E+00 0.5285953E+00
0.5819548E+00 0.6406503E+00 0.7052153E+00 0.7762369E+00 0.8543606E+00
0.9402966E+00 0.1034826E+01 0.1138809E+01 0.1253190E+01 0.1379009E+01
0.1517410E+01 0.1669651E+01 0.1837116E+01 0.2021328E+01 0.2223961E+01
0.2423961E+01 0.2623961E+01 0.2823961E+01 0.3023961E+01 0.3223961E+01
0.3423961E+01 0.3623961E+01 0.3823961E+01 0.4023961E+01 0.4223961E+01
0.4423961E+01 0.4623960E+01 0.4823960E+01 0.5023960E+01

2) Create bridge boundaries and model space

Input: mrcyl.txt

Output: mrcyl1.plt

Program: bgrid3.f

The output from the rdist.f program is used as the body of the mrcyl.txt file. An example below shows the 10 lines that are added to the beginning of the rdist.f output to produce the file mrcyl.txt.

mrcyl.txt

8,79

0.93548	3.2258e-2	5.0	5.0
1.0	0.0	5.0	0.0
.80645	-9.6774e-2	5.0	-5.0
0.19355	-9.6774e-2	-4.0	-5.0
0.0	0.0	-4.0	0.0
6.4516e-2	3.2258e-2	-4.0	5.0
0.5	4.3145e-2	0.5	5.0
0.93548	3.2258e-2	5.0	5.0

Boundary points around the bridge

Model space outside boundary points

21 25 90 25 21 45 45

The first line is the number of points creating the bridge boundary and the number of tangential grid points that were created by rdist.f. The next 8 lines contain the x and y coordinates of the bridge boundary in the first two columns and the coordinates defining the model space in the second two columns. The last line is the number of radial grid spacings along each line segment of the bridge boundary, which here equals 272.

The mrcyl.txt serves as the input file for the program bgrid3.f. This produces all the x-y coordinates of the grid points where calculations will be

made and outputs them to mrcyl1.plt. The first 6 lines are included below for clearer understanding.

mrcyl1.plt

VARIABLES = "X","Y"

ZONE I= 273 ,J= 79 ,F=POINT

0.9354800 3.2258000E-02

0.9385524 3.0721905E-02

0.9416248 2.9185809E-02

0.9446971 2.7649716E-02

The first line tells that the following data serve as x and y coordinates. The second line defines the grid points. The following lines contain all the data points for the grid line intersections, nodes.

3) Calculate coefficient of drag, lift, and vorticity

Input: f2d-i.txt

Output: f2d-o.plt & f2d-p.plt

Program: fdm2d2.out

The input file f2d-i.txt is the mrcyl1.plt file altered slightly. This .txt file contains all the grid data from the mrcyl1.plt file, but also contains the grid conditions, time duration, and Reynold's number in the first line. The following is the first10 lines of the f2d-i.txt file for Grid 1.

f2d-i.txt

273, 79, 20000, 1.e-5, 0.001

9.354800E-01 3.225800E-02

9.385524E-01 3.072190E-02

9.416248E-01 2.918581E-02

9.446971E-01 2.764971E-02

9.477695E-01 2.611362E-02

9.508419E-01 2.457752E-02

9.539143E-01 2.304143E-02

9.569867E-01 2.150533E-02

9.600590E-01 1.996924E-02

Definition of terms in first line:

radial nodes, # tangential nodes, # of time iterations, Reynold's number, duration of time step

The program fdm2d2.out is the determining factor in the amount of time for completion of the entire computer analysis, because it is the program that takes the most time to run. When it is completed there are two output files: f2d-o.plt and f2d-p.plt. When these two files are loaded into Tecplot, all the plots that are included in this work can be produced.

4) Coefficient of Drag

Input: fr-i.txt

Output: Average coefficient of drag

Program: aveg.exe

To determine the average coefficient of drag, the first 10 seconds of each run was cut from the f2d-o.txt file to allow for the calculations to regulate. This

new set of data becomes the input file fr-i.txt for the program aveg.exe. The number of lines the file contains is inserted as the first line and then the aveg.exe program can be run on any computer. The output from this program is the reported C_d. The first 5 lines from the fr-i.txt file are below.

fr-i.txt

29154

3.50011 0.5584026E-01 0.1110665E+00

3.50071 0.5581310E-01 0.1113747E+00

3.50132 0.5578360E-01 0.1116951E+00

3.50192 0.5575073E-01 0.1120265E+00

5) Frequency of the Coefficient of Lift

Input: fr-i.txt

Output: fr-o.plt

Program: freq3.exe

Typically the same amount of data is cut from the f2d-o.txt file to create the input file for the freq.exe program as is cut to create the input file for aveg.exe. If the same number of lines are cut, the fr-i.txt file can be used with a different first line. The first line for fr-i.txt for Grid 1 appears like the following:

fr-i.txt

17969, 10.00058, 20.00004, 1, 40, 2

The first number is the number of lines in the file following the first line. The next two numbers represent the start time and the end time of the data. The number 40 corresponds to the duration of time being analyzed but is not directly

proportional. It should be changed accordingly to account for the time duration of the data.

The output from this file is fr-o.txt ,which contains frequency and amplitude information. This file can be plotted using and Tecplot and from the plot the greatest amplitude frequencies can be found and used to calculate the Strouhal numbers.